Glutamates 99 and 107 in Transmembrane Helix III of Subunit I of Cytochrome *bd* Are Critical for Binding of the Heme b_{595}-*d* Binuclear Center and Enzyme Activity†

Tatsushi Mogi,*,‡,§ Sachiko Endou,§ Satoru Akimoto,§ Mayumi Morimoto-Tadokoro,§ and Hideto Miyoshi||

Chemical Resources Laboratory, Tokyo Institute of Technology, Nagatsuta 4259, Midori-ku, Yokohama 226-8503, Japan, ATP System Project, Exploratory Research for Advanced Technology, Japan Science and Technology Organization, Nagatsuta, Midori-ku, Yokohama 226-0026, Japan, and Division of Applied Life Sciences, Graduate School of Agriculture, Kyoto University, Sakyo-ku, Kyoto 606-8502, Japan

Received August 4, 2006; Revised Manuscript Received October 26, 2006

ABSTRACT: Cytochrome *bd* is a quinol oxidase of *Escherichia coli* under microaerophilic growth conditions. Coupling of the release of protons to the periplasm by quinol oxidation to the uptake of protons from the cytoplasm for dioxygen reduction generates a proton motive force. On the basis of sequence analysis, glutamates 99 and 107 conserved in transmembrane helix III of subunit I have been proposed to convey protons from the cytoplasm to heme *d* at the periplasmic side. To probe a putative proton channel present in subunit I of *E. coli* cytochrome *bd*, we substituted a total of 10 hydrophilic residues and two glycines conserved in helices I and III−V and examined effects of amino acid substitutions on the oxidase activity and bound hemes. We found that Ala or Leu mutants of Arg9 and Thr15 in helix I, Gly93 and Gly100 in helix III, and Ser190 and Thr194 in helix V exhibited the wild-type phenotypes, while Ala and Gln mutants of His126 in helix IV retained all hemes but partially lost the activity. In contrast, substitutions of Thr26 in helix I, Glu99 and Glu107 in helix III, Ser140 in helix IV, and Thr187 in helix V resulted in the concomitant loss of bound heme b_{558} (T187L) or b_{595}-*d* (T26L, E99L/A/D, E107L/A/D, and S140A) and the activity. Glu99 and Glu107 mutants except E107L completely lost the heme b_{595}-*d* center, as reported for heme b_{595} ligand (His19) mutants. On the basis of this study and previous studies, we propose arrangement of transmembrane helices in subunit I, which may explain possible roles of conserved hydrophilic residues within the membrane.

Cytochrome *bd* is one of two terminal ubiquinol oxidases in the aerobic respiratory chain of *Escherichia coli* and is predominantly expressed under microaerophilic growth conditions (see refs *1*−*3* for reviews). It catalyzes dioxygen reduction with two molecules of ubiquinol-8, leading to the release of four protons from quinols to the periplasm. Through a putative proton channel, four protons used for dioxygen reduction are taken up from the cytoplasm and delivered to the dioxygen reduction site at the periplasmic side of the cytoplasmic membrane (*4*). On the basis of sequence analysis, Osborne and Gennis (*5*) suggested that conserved Glu99 and Glu107 in helix III of subunit I are part of such a proton channel. Thus, cytochrome *bd* generates an electrochemical proton gradient across the membrane through apparent vectorial translocation of four chemical protons during dioxygen reduction (*6*−*8*). In contrast to cytochrome *bo*, an alternative ubiquinol oxidase under highly aerated growth conditions, cytochrome *bd* has no proton pumping activity and does not belong to the heme−copper terminal oxidase superfamily. Recently, it has been reported that cytochrome *bd* is involved in the survival and growth of strict anaerobes in oxic environments (*9*−*11*) and in the virulence and survival of pathogenic bacteria in host mammalian cells (*12*−*14*).

Cytochrome *bd* has been isolated as a heterodimeric oxidase [CydAB in *E. coli* (*6*, *15*, *16*)] and is distributed from archaea to eubacteria. On the basis of spectroscopic and ligand binding studies, three distinct redox metal centers have been identified as heme b_{558}, heme b_{595}, and heme *d* (see ref *17* for a review). Unlike cytochrome *bo*, cytochrome *bd* does not contain a tightly bound ubiquinone-8. Heme b_{558} is a low-spin protoheme IX and is ligated by His186 (helix V) and Met393 (helix VII) of subunit I (CydA) (*18*, *19*) (Figure 1A). Reduced heme b_{558} has absorption peaks at 428, 531, and 561 nm at room temperature. Inhibitor binding studies indicate the proximity of heme b_{558} to the quinol oxidation site (*21*, *22*). Heme b_{595} is a high-spin protoheme IX bound to His19 (helix I) of subunit I (*18*) and mediates electron transfer from heme b_{558} to heme *d* (*23*−*25*), where dioxygen is reduced to water. Reduced heme b_{595} exhibits absorption peaks at 440, 560, and 596 nm. Heme *d* is a high-spin chlorin and forms a diheme binuclear center with heme b_{595} (*26*−*28*). Heme *d* exhibits the α peak at 630 nm in the fully reduced form and at 646 nm in the air-oxidized, oxygenated form. Resonance Raman studies (*29*, *30*) indi-

† This work was supported in part by a Grant-in-Aid for Scientific Research from the Japan Society for the Promotion of Science (15380083 to H.M.).

* To whom correspondence should be addressed: Sogokenkyukan-Bekkan, Tokyo Institute of Technology, Nagatsuta 4259, Midori-ku, Yokohama 226-8503, Japan. Telephone: +81-45-922-5238. Fax: +81-45-922-5239. E-mail: tmogi@res.titech.ac.jp.

‡ Tokyo Institute of Technology.

§ Japan Science and Technology Organization.

|| Kyoto University.

10.1021/bi0615792 CCC: $33.50
Published on Web 12/08/2006

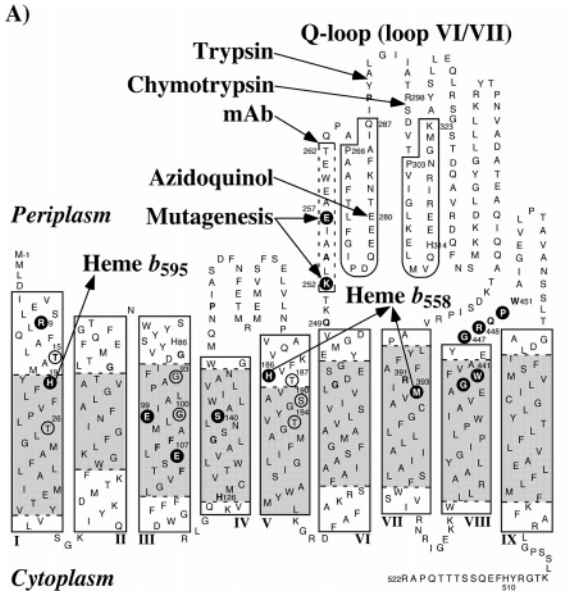

B)

Helix I	
Arg9	155 Arg, 1 ND
Thr15	136 Thr, 7 Ser, 6 Val, 5 Phe, 2 Asn
His19	156 His
Thr26	106 Thr, 33 Ser, 15 Gly, 3 Asn
Helix III	
His86	57 His, 26 Arg, 11 Lys, 19 Glu, 43 Others
Gly93	141 Gly, 12 Ala, 2 Ser, 1 Val
Glu99	151 Glu, 5 Xaa
Gly100	75 Gly, 37 Ala, 26 Val, 4 Thr, 14 ND
Glu107	151 Glu, 5 Xaa
Helix IV	
His126	140 His, 9 Arg, 6 Tyr, 1 Lys
Ser140	155 Ser, 1 Xaa
Helix V	
His186	156 His
Thr187	72 Thr, 38 Met, 9 Xaa, 27 Val, 8 Ala, 2 Ser
Ser190	46 Ser, 14 Thr, 61 Ala, 34 Gly, 1 Val
Thr194	90 Thr, 15 Ser, 5 Cys, 8 Ala, 38 Others

FIGURE 1: (A) Topological model and (B) amino acid residues found at relevant positions of subunit I. (A) Transmembrane helices and hydrophobic segments were predicted by PSIpred (http://bioinf.cs.ucl.ac.uk/psipred/) and SOSUI (http://sosui.proteome.bio.tuat.ac.jp/sosuiframe0.html), respectively, and represented by rectangles and gray highlighting, respectively. In contrast, the new joint method (*43*) (http://mbs.cbrc.jp/papia-cgi/ssp_menu.pl) predicts the presence of two short α-helices [I_N (Met1−Phe22) and I_C (Leu25−Leu42)] in helix I and an additional helix (Glu162−Lys183) between helices IV and V. Fourteen invariant residues are highlighted, and highly conserved residues are in bold. His19 serves as the axial ligand for heme b_{595}, and His186 and Met393 serve as the axial ligands for heme b_{558}, which accepts electrons from quinols. Mutagenized residues other than Arg9 are encircled. The epitope for mAb, proteolytic cleavage sites, and the azidoquinol-cross-linked site in Q-loop are denoted with arrows. The Glu257−Met347 region in the Q-loop contains internal repeats (Pro266−Gln287 and Pro303−Lys323) and shows a weak similarity (23.1% identical) to the C-terminal tail domain of moesin, which binds F-actin and the N-terminal FERM (band 4.1 protein and ezrin/radixin/moesin homology) domain in eukaryotic cells (*20*). The numbering of amino acid residues is that of Zhang et al. (*4*). (B) One hundred fifty-six of 212 subunit I sequences in the GTOP database (http://spock.genes.nig.ac.jp/~genome/gtop-j.html) have all three ligands for heme b_{558} and b_{595} and are used for sequence analysis.

cated the axial ligand of heme *d* would not be an ordinary histidine or cysteine and is either a weakly coordinating protein donor or a water molecule. Electron nuclear double-resonance studies (*31*) also suggested that heme *d* does not contain a nitrogenous ligand. When dioxygen binds, the axial ligand apparently dissociates from heme *d* and remains off in the formation of the oxoferryl state (*30*). On the other hand, electron paramagnetic resonance studies with NO as a monitoring probe showed that the proximal ligand of heme *d* is a histidine in an anomalous condition or other nitrogenous amino acid residue (*26*). Topological analysis suggests that all the hemes are located at the periplasmic side of transmembrane helices (*4*). Electron paramagnetic resonance studies indicate that heme b_{558} and heme *d* are oriented with their heme planes perpendicular to the membrane plane, whereas heme b_{595} is oriented with its heme plane at an angle of ~55° to the membrane plane (*32*).

To understand the energy transduction mechanism of cytochrome *bd*, it is essential to identify the quinol oxidation site (proton release site) at the periplasmic side of the cytoplasmic membrane and the heme *d*-binding site (proton uptake site) connecting to the cytoplasm through a putative proton channel. In loop VI−VII (Q-loop) of subunit I, binding of monoclonal antibodies to ^{252}KLAAIEAEWET^{262} (*33*, *34*) and proteolytic cleavage with trypsin at Tyr290 or chymotrypsin at Arg298 (*35*, *36*) suppressed ubiquinol oxidase activity (Figure 1A). Photoaffinity labeling studies with azidoquinols identified that Glu280 is a part of the binding pocket for 2- and 3-methoxy groups on the ubiquinone ring (*37*). Site-directed mutagenesis studies indicated that Lys252 and Glu257 are involved in the quinol oxidation by cytochrome *bd* (*38*). These observations indicate the presence of the quinol oxidation site in the N-terminal region of Q-loop.

In contrast to the quinol oxidation site, the heme *d* ligand still remains to be determined. Fourteen strictly conserved residues in cytochrome *bd* are all present in subunit I (Figure 1A). Possible nitrogenous heme *d* ligands are Arg9, His126, and Arg448. However, mutagenesis studies (*18*, *39*) eliminated the possible role of the latter two residues. To probe a putative proton channel in subunit I connecting heme *d* to the cytoplasm, we examined effects of substitutions of 10 hydrophilic residues in helices I and III−V and two glycines in helix III (Figure 1B) on the oxidase activity and heme binding. We found that Glu99 and Glu107 in helix III are essential for binding of the heme b_{595}-*d* binuclear center and the enzyme activity. On the basis of this and previous studies, we propose arrangement of transmembrane helices in subunit I, which may explain possible roles of conserved Glu99, Glu107, His126, and Ser140.

EXPERIMENTAL PROCEDURES

Mutagenesis and Expression of Cytochrome bd. Amino acid substitutions were introduced with QuickChange XL (Stratagene) using pNG2 (*cyd*$^+$ Tet^R) (*40*) and synthetic oligonucleotides (Table S1). Thr15, Thr26, Thr187, and Thr194 were substituted with Leu, Arg9, Gly93, Gly100, Ser140, and Ser190 with Ala, and Glu99 and Glu107 with Leu, Ala, and Asp, and His126 was substituted with Ala and Gln and Glu280 with Asp. Mutations were confirmed by DNA sequencing. For isolation of defective mutant enzymes, ST4683/pMFO9 (Δ*cyo*::Cm^R Δ*cyd*::Km^R/*cyo*$^+$ Amp^R) was

transformed with mutant pNG2, and transformants were aerobically grown overnight in IM medium supplemented with 0.5% glucose, 12.5 μg/mL tetracycline, and trace metals (*38*). R9A, T15L, T26L, H126A, H126Q, S140A, T194L, and E280D were expressed in ST4683 harboring mutant pNG2 plasmids.

Isolation of Mutant Cytochrome bd. Cells were suspended in 50 mM Tris-HCl (pH 7.4) containing 10 mM Na-EDTA, 1 mM phenylmethanesulfonyl fluoride (Sigma) and 0.5 mg/mL lysozyme (Sigma) and disrupted by sonication. Enzymes were solubilized from cytoplasmic membranes with 2.5% (w/v) sucrose monolaurate (SML)[1] (Mitsubishi-Kagaku Foods Co., Tokyo, Japan) and purified by anion-exchange high-performance liquid chromatography on a TSKgel SuperQ-5PW column [21.5 mm (inside diameter) × 15 cm; Tosoh, Tokyo, Japan] in 50 mM sodium phosphate (pH 6.8) containing 0.1% (w/v) SML and 0.1 mM phenylmethanesulfonyl fluoride (*38*). Defective mutant enzymes were further purified by rechromatography or as the flow-through fraction by passing through a Ni-NTA His-Bind Superflow (Novagen) column. Purified enzymes were concentrated to ~50 mg/mL by ultrafiltration with Amicon Ultra-15 (MWCO of 50 kDa) and stored at −80 °C until they were used.

Determination of Heme and Protein Content. Heme B content was determined with the pyridine hemochromogen method, and heme D content was estimated from redox difference spectra using a molar extinction coefficient ($\epsilon_{628-651}$) of 27 900 (*41*). Protein concentrations were determined by the BCA method (Pierce).

Absorption Spectroscopy. Absorption spectra of the air-oxidized and sodium hydrosulfite-reduced forms of mutant enzymes were determined with a V-550 UV−vis spectrophotometer (JASCO, Tokyo, Japan) at a final concentration of 10 μM in 50 mM sodium phosphate (pH 7.4) containing 0.1% SML.

Spectroscopic Assay of Quinol Oxidase Activity. Quinol oxidase activity was determined at 25 °C by monitoring the absorbance change at 278 nm and calculated using an extinction coefficient of 12 300 (*42*). The reaction mixture (1 mL) contained 50 mM sodium phosphate (pH 7.4), 0.1% SML, and 12.5−125 nM purified cytochrome *bd*. The enzyme concentration was estimated from the heme B content, by assuming that cytochrome *bd* contains two *b* hemes. The reaction was started by the addition of a reduced form of ubiquinone-1, a kind gift from Eisai Co. (Tokyo, Japan), at a final concentration of 200 μM. For kinetic analysis, the concentration of ubiquinol-1 was varied from 33 to 400 μM. K_m and V_{max} values were estimated with Kaleidagraph version 3.5 (Synergy Software).

Polarographic Assay of Oxidase Activity. Oxygen consumption was assessed with a YSI model 5300 biological oxygen monitor (YSI Inc., Yellow Springs, OH) in a closed stirred glass vessel (3 mL) at 25 °C. Reaction was started by the addition of 30 μL of the enzymes (100 μM heme B) to 2.97 mL of 100 mM sodium phosphate (pH 7.4) containing 0.1% SML, 0.2 mM TMPD (*N*,*N*,*N*′,*N*′-tetramethyl-*p*-phenylenediamine), and 5 mM sodium ascorbate. The dissolved oxygen concentration at 25 °C was assumed to be 237 μM.

Aerobic Reduction of Cytochrome bd by Ubiquinol-1. To enzyme solutions (10 μM heme B) in 50 mM sodium phosphate (pH 7.4) containing 0.1% SML were added ubiquinol-1 and dithiothreitol to a final concentration of 200 μM and 5 mM, respectively. Absorbance changes at 561 and 630 nm were monitored at 25 °C with a V-550 UV−vis spectrophotometer.

RESULTS

Properties of Helix I Mutants. Subunit I (CydA) consists of nine transmembrane helices with the N-terminus in the periplasm (*4*). One hundred fifty-six of 212 CydA sequences in the GTOP database have all three ligands for heme b_{558} (His186 and Met393) and b_{595} (His19) (Figure 1B), so we assumed that their cytochrome *bd* is functionally expressed. Among them, Arg9, Thr15, His19, and Thr26 are conserved in helix I. In our structure model for subunit I, Arg9, Thr15, and His19 face the periplasm whereas Thr26 is completely embedded within the membrane (Figure 1A).

All the helix I mutations on plasmid pNG2 complemented a defect of the aerobic growth of the quinol oxidase-deficient mutant ST4683 (Δ*cyo* Δ*cyd*), indicating that the mutant oxidases retain the enzyme activity. We characterized cytoplasmic membranes and enzymes and found that R9A and T15L did not affect the heme binding and oxidase activity (Table 1 and Figure 2B). T26L reduced the level of heme *d* binding and the oxidase activity to approximately half of the wild-type level. Absorption spectra of the air-oxidized (as-prepared) and fully reduced forms of T26L showed the decrease in the peak intensity at 440, 596, 627, and 640 nm (Figure 2C and Table S2), indicating the loss of the heme b_{595}-*d* binuclear center.

By assuming the ping-pong bi-bi mechanism, we carried out kinetic analysis of the oxidation of ubiquinol-1 by mutant enzymes and determined kinetic parameters without or with substrate inhibition by using eq 1 or 2, respectively (*44*).

$$v = \frac{V_{max}[S]^2}{K_m{}^2 + K_m[S] + [S]^2} \quad (1)$$

$$v = \frac{V_{max}[S]^2}{K_m{}^2 + K_m[S] + \left[1 + \left(\frac{[S]}{K_i}\right)^n\right][S]^2} \quad (2)$$

where K_i and n are the constant for substrate inhibition and the Hill coefficient, respectively. In contrast to the quinol oxidation site (Q-loop) mutants (ref *36* and E280D in Table 2), which showed the increase in K_m, T26L exhibited a 2-fold decrease in K_m and a 4-fold decrease in V_{max}, which were associated with substrate inhibition (Table 2 and Figure 3B).

Properties of Helix III Mutants. In cytochrome *bd*, Glu99 and Glu107 are strictly conserved in the middle of transmembrane helix III (Figure 1A) and are likely candidates for key residues in the proton uptake channel (*5*). Because of small side chain size, Gly93 and Gly100 may form a pathway connecting the periplasm to Glu99 (Figure 1A). We expressed helix III mutants in cytochrome *bo*-expressing strain ST4683/pMFO9 (Δ*cyo* Δ*cyd*/*cyo*$^+$) harboring mutant pNG2 and found that G93A and G100A exhibited the wild-

[1] Abbreviations: SML, sucrose monolaurate; TMPD, *N*,*N*,*N*′,*N*′-tetramethyl-*p*-phenylenediamine.

Table 1: Heme Contents and Oxidase Activity of Mutant Cytochrome *bd*

		cytoplasmic membranes			isolated cytochrome *bd*			
		heme content (nmol/mg of protein)			heme content (nmol/mg of protein)			
location in subunit I		heme *b*	heme *d*	heme *d*/heme *b*	heme *b*	heme *d*	heme *d*/heme *b*	oxidase activity (Q_1H_2/s)[b]
	wild type	4.28	1.96	0.46	13.1	6.28	0.48	234
helix I	R9A[a]	4.47	2.03	0.45	10.8	5.67	0.53	252
	T15L[a]	4.25	2.15	0.51	13.3	5.54	0.42	236
	T26L[a]	4.82	1.47	0.30	13.1	3.86	0.29	99.3
helix III	G93A	4.85	1.99	0.41	16.4	7.22	0.44	262
	E99L	4.85	<0.01	<0.01	11.4	0.19	0.02	16.1
	E99A	1.07	<0.01	<0.01	1.81	0.01	<0.01	29.5
	E99D	1.25	<0.01	<0.01	1.44	<0.01	<0.01	1.3
	G100A	4.89	2.53	0.52	17.1	8.41	0.49	238
	E107L	5.03	0.98	0.19	16.9	4.89	0.29	19.8
	E107A	1.37	<0.01	<0.01	1.26	0.03	0.02	8.7
	E107D	1.44	<0.01	<0.01	1.52	0.06	0.04	19.8
helix IV	H126A[a]	5.24	2.58	0.49	16.6	8.20	0.49	82.8
	H126Q[a]	4.81	2.39	0.50	18.1	8.75	0.48	82.1
	S140A[a]	5.63	2.78	0.49	16.7	5.17	0.31	139
helix V	T187L	3.89	1.86	0.48	10.7	6.64	0.62	100
	S190A	4.96	2.40	0.48	17.7	9.08	0.51	238
	T194L[a]	5.25	2.77	0.53	16.6	8.16	0.49	267
loop VI−VII	K252A[c]	5.15	2.39	0.46	18.2	8.20	0.45	8.3
	E280D[a]	4.81	2.48	0.52	17.7	8.87	0.50	8.0

[a] Expressed in ST4683 harboring mutant pNG2. Other mutants were expressed in ST4683/pMFO9 harboring pNG2. [b] Oxidase activity was determined with 200 μM ubiquinol-1 and expressed as the turnover number by assuming that all the mutant enzymes contain two *b* hemes. Because of the difficulty in estimating heme *d* content in Glu99 and Glu107 mutants, the specific activity per heme *d* gave erroneous estimates. [c] Data taken from ref *38*.

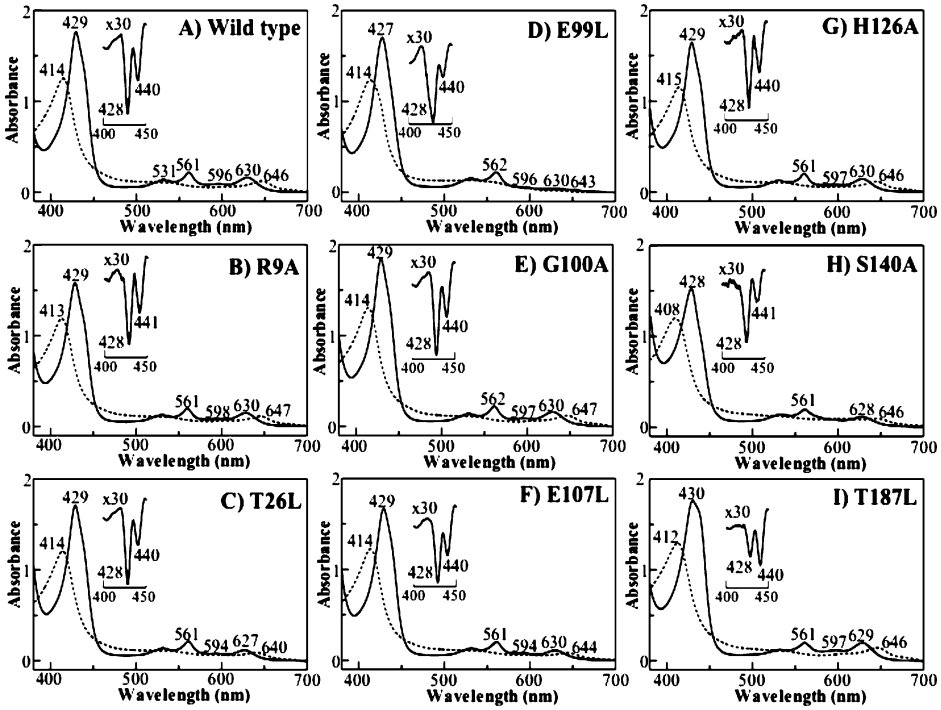

FIGURE 2: Absorption spectra of the air-oxidized (as-prepared) (- - -) and fully reduced (—) forms of subunit I mutants. Absolute spectra of the isolated enzymes were recorded in 50 mM sodium phosphate (pH 7.4) containing 0.1% SML before (- - -) and after reduction (—) with sodium hydrosulfite. The enzyme concentration was 20 μM heme B. The insets show the second-order finite difference spectra for the Soret peak.

type phenotypes (Table 1), indicating that both Gly93 and Gly100 are dispensable for the catalytic functions.

In contrast, Glu99 and Glu107 mutations severely reduced the oxidase activity and eliminated heme *d* binding except E107L (Table 1). Visible absorption spectra for E99L and E107L showed that the decrease in the peak intensity at 630 and 640 nm originating from ferrous and oxygenated heme *d*, respectively, was accompanied by a decrease in the peak intensity at 440 and 595 nm originating from ferrous heme b_{595} (Figure 2D,F). Kinetic analysis of the oxidation of ubiquinol-1 by E107L, which retains 60% of heme *d*, revealed the large decrease in V_{max} (5% per two *b* hemes or 9% per heme *d*) (Table 2 and Figure 3B). Replacement of strictly conserved Glu99 and Glu107 with Asp resulted in nonfunctional enzymes, as found for Glu280 at the quinol oxidation site (Table 1). Thus, not only negative charge but

Table 2: Kinetic Parameters for Oxidation of Ubiquinol-1 by Isolated Subunit I Mutants

	K_m (μM)	V_{max} (Q_1H_2/s)	V_{max}/K_m (Q_1H_2 s^{-1} μM^{-1})	K_i (μM)	*n*
wild type	123	445 (464)[a]	3.62 (100)[b]	*c*	*c*
R9A	47	566 (539)[a]	12.0 (333)[b]	301	1.5
T26L	53	112 (190)[a]	2.11 (58)[b]	464	4.0
G93A	96	442 (502)[a]	4.60 (127)[b]	481	5.9
G100A	103	400 (407)[a]	3.88 (107)[b]	*c*	*c*
E107L	34	24 (41)[a]	0.71 (20)[b]	569	4.6
H126Q	36	319 (330)[a]	8.86 (245)[b]	200	4.5
S140A	18	143 (231)[a]	7.94 (219)[b]	336	3.7
T187L	84	160 (129)[a]	1.90 (52)[b]	*c*	*c*
E280D	1356	545 (544)[a]	0.40 (11)[b]	50	2.1

[a] V_{max} values per heme *d* are given in parentheses. [b] No substrate inhibition.

also side chain size is important at these positions. A residual activity found in defective enzymes like E99L may be partly due to the contribution from the heme *bbb*-type enzyme, which has been shown to be functional in *Bacillus subtilis* (*44*) and in CIO (cyanide-insensitive oxidase) from *Pseudomonas aeruginosa* (*45*) and other bacteria (*46*).

Properties of Helix IV Mutants. His126 and Ser140 are highly conserved in helix IV (Figure 1B) and may be involved in proton uptake channel. We found that all three mutations on plasmid pNG2 complemented the defect of the aerobic growth of ST4683, indicating that His126 and Ser140 are not essential for activity. H126A and H126Q bind all three hemes but reduced the oxidase activity to 60 and 70%, respectively, of the control level (Table 1 and Figure 2G). S140A showed an ~40% decrease in oxidase activity and the heme b_{595}-*d* binuclear center (Table 1 and Figure 2H). Kinetic analysis of helix IV mutants revealed the decrease in both K_m and V_{max}, which was accompanied by substrate inhibition (Table 2).

Properties of Helix V Mutants. Thr187, Ser190, and Thr194 are not well-conserved in subunit I (Figure 1B), but they could provide a hydrophilic pathway on helix V connecting the periplasm to heme b_{558}, which is bound to His186. To test their possible roles in oxidase activity, we constructed T187L, S190A, and T194L mutants and expressed T187L and S190A mutations in ST4683/pMFO9/pNG2 and the T194L mutation in ST4683/pNG2. We found that S190A and T194L were fully active, whereas T187L reduced the heme *b* content and oxidase activity to 80 and 43%, respectively, of the wild-type levels (Table 1). Spectroscopic analysis of the fully reduced T187L revealed a partial loss of heme b_{558}, indicated by the decreased peak intensity at 428 and 561 nm (Figure 2I). If we could assume that the heme b_{595}-*d* center in T187L is intact, a relative content of heme b_{558} will be 0.62 per heme *d* (i.e., 4.1:6.6:6.6 b_{558}:b_{595}:*d*). Our observations suggest that Thr187, Ser190, and Thr194 in helix V are dispensable for the catalytic function.

Ascorbate/TMPD-Dependent Oxygen Consumption by E107L. Effects of the E107L mutation on the oxygen uptake by the heme b_{595}-*d* binuclear center were examined polarographically. By assuming that two heme B molecules are bound to the mutant enzymes, we estimated the ascorbate/TMPD oxidase activity. Reduced TMPD can donate electrons to hemes from a site after the quinol oxidation site (*35*). K252A and E280D (the quinol oxidation site mutants) exhibited 70−80% of the wild-type activity, while E107L reduced the oxygen uptake activity to 19% (per two *b* hemes) or 31% (per heme *d*) of the wild-type level, indicating the defect at the heme b_{595}-*d* binuclear center.

Aerobic Reduction of E107L by Ubiquinol-1. Recently, Zhang et al. (*48*) reported that anaerobic reduction of cytochrome *bd* by ubiquinol-1 and dithiothreitol was very slow and not to be related to the catalytic function. Thus, to probe effects of the E107L mutation on the transfer of electrons from quinols to hemes, we examined aerobic reduction of mutant enzymes (10 μM heme B) with 200 μM ubiquinol-1 in the presence of 5 mM dithiothreitol, which can keep substrates as a reduced form. The aerobic reduction of hemes was monitored at 561 (heme b_{558}^{2+} and b_{595}^{2+}) and 630 nm (heme d^{2+}). As reported previously (*49*), the wild-type enzyme showed a rapid reduction of *b* hemes, followed by the reoxidation with dioxygen and a re-reduction after the depletion of dioxygen in the reaction medium (Figure 4A). The time course of heme *d* reduction at 630 nm indicates that transfer of an electron from heme b_{595} to heme *d* is not the rate-limiting step for heme *d* reduction with quinols (Figure 4B). K252A, the quinol oxidation site mutation (*38*), suppressed the reoxidation and re-reduction of both hemes *b* and *d* because of a slow electron supply from ubiquinol-1 to heme b_{558}. In E107L (heme *d*/heme *b* = 0.29), the amplitude of heme *b* re-reduction was much larger than that for heme *d*. This may be partly due to the contribution of the heme b_{595}-*d*-deficient population, where heme b_{558} may have the altered E_m value and would not be oxidized with dioxygen. It is also possible that reduction of heme b_{595} requires charge compensation with a supply of chemical protons, from a protonatable group at the cytoplasmic side of the heme b_{595}-*d* binuclear center (*49*). This portion could correspond to the heme *d* re-reduction, which is coupled to the electron supply from heme b_{595} (*23*−*25*). In contrast to the wild type and K252A, two-thirds of heme *d* in E107L remains reduced. Because of the absence of proteinaceous counter charges within the membrane, both Glu99 and Glu107 are likely protonated, which is indicated by FTIR studies (*50*). The direct electron donor to heme *d* must be still present in E107L, allowing the reduction of heme *d*. But the slow supply of chemical protons from the channel and electron from heme b_{595} would suppress dioxygen reduction. Glu99 and Glu107, which have been suggested to be involved in the proton uptake channel (*5*), may play such a crucial role in the dioxygen reduction by cytochrome *bd*. Future work is needed to address this issue.

DISCUSSION

To understand the energy transduction mechanism of cytochrome *bd*, it is essential to identify the proton release site (quinol oxidation site) and the proton uptake site (heme *d*-binding site), which are expected to be at the periplasmic and cytoplasmic side, respectively, of the cytoplasmic membrane. Topology studies placed all three axial ligands for heme b_{558} and b_{595} at the periplasmic ends of transmembrane helices in subunit I (*4*). Since heme *d* forms the diheme binuclear center with heme b_{595} (*26*−*28*), all three hemes appear to be located at the periplasmic side. Thus, the role of proton uptake channel connecting heme *d* to the cytoplasm is important for the dioxygen reduction at the heme b_{595}-*d* binuclear center.

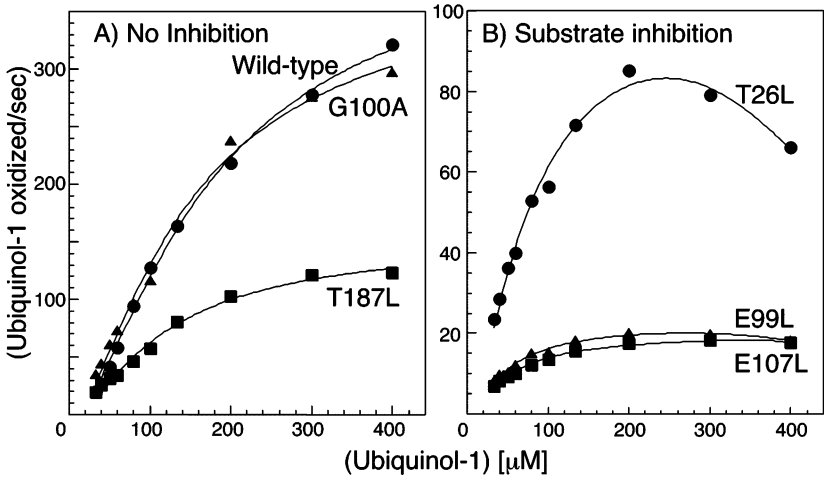

FIGURE 3: Dependence of ubiquinol oxidation by subunit I mutants on the ubiquinol-1 concentration. (A) Without substrate inhibition: wild type (●), G100A (▲), and T187L (■). (B) With modest substrate inhibition: T26L (●), E99L (▲), and E107L (■). Curve fitting was carried out with Kaleidagraph by using eq 1 or 2.

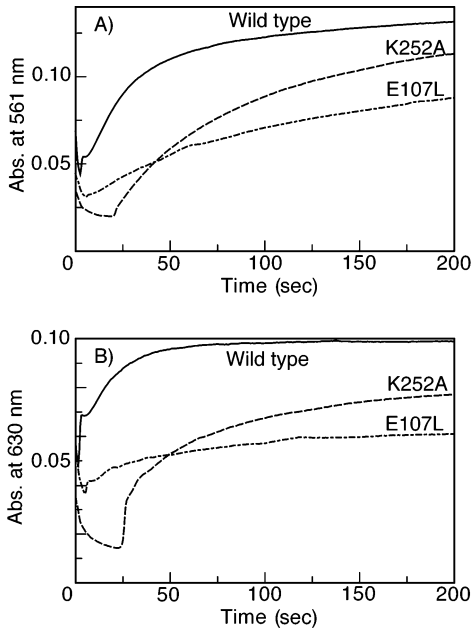

FIGURE 4: Time course of aerobic reduction of *b* hemes (A) and heme *d* (B) in mutant enzymes. Aerobic reduction of the mutant enzymes (10 μM heme B) was carried out at 25 °C in the presence of 200 μM ubiquinol-1 and 5 mM dithiothreitol and monitored at 561 and 630 nm.

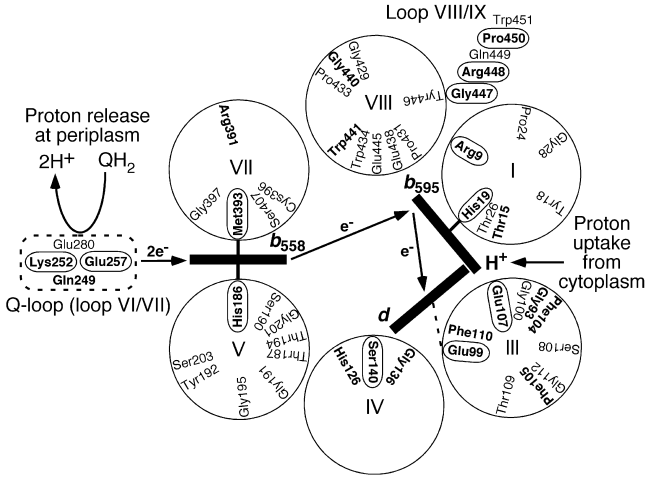

FIGURE 5: Helical wheel projection model for the reaction center on subunit I. Invariant residues are encircled, and highly conserved residues are in bold. Electrons are transferred from the quinol oxidation site in the Q-loop to heme *d* through heme b_{558} and b_{595}. Protons used for dioxygen reduction are taken up from the cytoplasm through a proton channel where Glu99 and Glu107 are assumed to mediate the proton translocation. Spontaneous mutations in subunit II (*51*) and proximity mapping studies using an artificial protease (*52*) indicated that helices I and II of subunit II are close to the Q-loop of subunit I.

Quinol Oxidation Site in Loop VI/VII (Q-loop). Binding of monoclonal antibodies to ^{252}KLAAIEAEWET^{262} (*33*, *34*) and proteolytic cleavage at Tyr290 or Arg298 (*35*, *36*) suppressed ubiquinol oxidase activity, indicating the presence of the quinol oxidation site in Q-loop (Figure 1A). Via photoaffinity labeling studies with azidoquinols, we have recently demonstrated that Glu280 in the first internal repeat is a part of the binding pocket for 2- and 3-methoxy groups on the ubiquinone ring (*37*). Further, we have identified by site-directed mutagenesis that conserved Lys252 and Glu257 in the N-terminal region are involved in the binding and oxidation of quinols (*38*). Accordingly, the binding site for the quinone ring is comprised of Lys252, Glu257, and Glu280 in the Q-loop and serves as a proton release site of cytochrome *bd* (Figure 5). In addition, Zhang et al. (*39*) demonstrated the importance of conserved Trp441 and Glu445 in helix VIII and Arg448 and Trp451 in loop VIII−IX in the oxidase activity. R448A reduced the level of heme *d* binding (*39*), and E445A kept heme b_{595} in a ferric state even with excess hydrosulfite (*49*). Belevich et al. (*49*) suggested that Glu445 is one of the two redox-linked protonatable groups required for charge compensation of the heme b_{595}-*d* binuclear center upon its two-electron reduction.

Structure of the Heme b_{595}-d Binding Site. Electron nuclear double-resonance studies (*31*) suggested that heme *d* does not contain a nitrogenous ligand. Resonance Raman studies (*29*, *30*) indicated the axial ligand of heme *d* would not be an ordinary histidine or cysteine and is either a weakly coordinating protein donor or a water molecule. Histidine mutagenesis studies on subunits I and II (*18*) showed that H19L and H19R eliminated the heme b_{595}-*d* binuclear center while H186L resulted in a loss of heme b_{558}. In addition, His126 in helix IV could be substituted with Arg, Thr, or Leu and His314 in the second internal repeat of the Q-loop

with Leu (*18*), and we show here that Arg9 and His126 cannot be the axial ligand of heme *d*. On the basis of spectroscopic properties (*29*−*31*), His19 and His186 in subunit I can be assigned to axial ligands for heme b_{595} and b_{558}, respectively. Methionine mutagenesis studies on subunit I identified Met393 as an additional ligand to heme b_{558} (*19*). Substitutions of nearby Arg391 did not affect the heme binding but induced an ~220 mV decrease in the midpoint potentials of heme b_{558}, indicating that a positive charge at Arg391 stabilizes the reduced form of heme b_{558} (*48*).

In cytochrome *bd*, there are only 14 strictly conserved residues, which are all present in subunit I (Figure 1). Spectroscopic and mutagenesis studies indicate that the axial ligands of heme *d* cannot be histidines, cysteines, methionines, or arginines (i.e., Arg9, Arg391, and Arg448). One of the possible ligands could be carboxylates (*30*). With the exception of His19 mutations (*18*), only substitutions of Glu99 eliminated the heme b_{595}-*d* binuclear center. A possible role of Glu99 in helix III as a weakly coordinating ligand to heme *d* (Figure 5) needs to be tested in a future study.

Effects of mutations on the heme binding and oxidase activity (*18*, *19*, *38*, *39*, *48*, *49*) (Figure 2 and Table 1) and the formation of the heme b_{595}-*d* binuclear center (*26*−*28*) suggest that helices V and VII form the heme b_{558}-binding site and helices I, III, IV, and VIII of subunit I would provide a binding pocket for the heme b_{595}-*d* binuclear center (Figure 5). Fourier transform infrared studies on cytochrome *bd* revealed three redox-sensitive bands in the protonated carboxylic C−O stretching region (+1752/−1760, +1731/−1738, and +1720/−1726 cm^{-1}) and one redox-sensitive band in the Cys−SH stretching region (+2562/−2570 cm^{-1}), indicating the hydrogen bonding is strengthened upon reduction (*50*). Notably, CN binding reduced the intensity of the positive 1752 cm^{-1} band originating from a carboxy residue buried in a nonpolar environment (*50*). The proximity of Glu99 and Glu107 in helix III and Glu445 in helix VIII to the heme b_{595}-*d* binuclear center indicates that they are likely candidates for the redox-sensitive carboxy residues. A redox-sensitive cysteine could be tentatively assigned to Cys396 on helix VII, one turn away from the heme b_{558} ligand (Met393). As postulated by Osborne and Gennis (*5*), Glu99 and Glu107 likely mediate the translocation of chemical protons from the cytoplasm to heme *d*. One of them may serve as the protonatable group (X_N^-) at the cytoplasmic side of the heme b_{595}-*d* binuclear center (*49*). In addition, the decrease in V_{max} for H126Q and S140A mutants may indicate the involvement of His126 and Ser140 in helix IV in proton translocation.

In conclusion, site-directed mutagenesis studies on transmembrane helices I and III−V of subunit I revealed that Glu99 and Glu107 in helix III are critical for the oxidase activity and binding of the heme b_{595}-*d* binuclear center. These conserved glutamates within the membrane have been suggested to facilitate translocation of chemical protons from the cytoplasm to the heme b_{595}-*d* binuclear center (*5*). We hope that future X-ray crystallographic and time-resolved spectroscopic studies would provide insight into the understanding of the molecular mechanism for the vectorial translocation of chemical protons by cytochrome *bd*-type terminal oxidase.

ACKNOWLEDGMENT

We thank R. B. Gennis (University of Illinois, Urbana, IL) for pNG2, Eisai Co. (Tokyo, Japan) for ubiquinone-1, K. Kita (University of Tokyo, Tokyo, Japan) for his help with the polarographic assay, and T. Yano (Japan Science and Technology Organization) for his comments on the manuscript.

SUPPORTING INFORMATION AVAILABLE

Table S1 and Table S2 show oligonucleotides used for site-directed mutagenesis and spectroscopic properties of mutant oxidases, respectively. This material is available free of charge via the Internet at http://pubs.acs.org.

REFERENCES

1. Ingledew, W. J., and Poole, R. K. (1984) The respiratory chain of *Escherichia coli*, *Microbiol. Rev. 48*, 222−271.
2. Jünemann, S. (1997) Cytochrome *bd* terminal oxidase, *Biochim. Biophys. Acta 1321*, 107−127.
3. Mogi, T., Tsubaki, M., Hori, H., Miyoshi, H., Nakamura, H., and Anraku, Y. (1998) Two terminal quinol oxidase families in *Escherichia coli*: Variations on molecular machinery for dioxygen reduction, *J. Biochem. Mol. Biol. Biophys. 2*, 79−110.
4. Zhang, J., Barquera, B., and Gennis, R. B. (2004) Gene fusions with β-lactamase show that subunit I of the cytochrome *bd* quinol oxidase from *E. coli* has nine transmembrane helices with the O_2 reactive site near the periplasmic surface, *FEBS Lett. 561*, 58−62.
5. Osborne, J. P., and Gennis, R. B. (1999) Sequence analysis of cytochrome *bd* oxidase suggests a revised topology for subunit I, *Biochim. Biophys. Acta 1410*, 32−50.
6. Kita, K., Konishi, K., and Anraku, Y. (1984) Terminal oxidases of *Escherichia coli* aerobic respiratory chain. II. Purification and properties of cytochrome b_{558}-*d* complex from cells grown with limited oxygen and evidence of branched electron-carrying systems, *J. Biol. Chem. 259*, 3375−3381.
7. Miller, M. J., and Gennis, R. B. (1985) The cytochrome *d* complex is a coupling site in the aerobic respiratory chain of *Escherichia coli*, *J. Biol. Chem. 260*, 14003−14008.
8. Jasaitis, A., Borisov, V. B., Belevich, N. P., Morgan, J. E., Konstantinov, A. A., and Verkohsky, M. I. (2000) Electrogenic reactions of cytochrome *bd*, *Biochemistry 39*, 13800−13809.
9. Lemos, R. S., Gomes, C. M., Santana, M., LeGall, J., Xavier, A. V., and Teixeira, M. (2001) The 'strict' anaerobe *Desulfovibrio gigas* contains a membrane-bound oxygen-reducing respiratory chain, *FEBS Lett. 496*, 40−43.
10. Baughn, A. D., and Malamy, M. H. (2004) The strict anaerobe *Bacteroides fragilis* grows in and benefits from nanomolar concentrations of oxygen, *Nature 427*, 441−444.
11. Lin, W. C., Coppi, M. V., and Lovley, D. R. (2004) *Geobacter sulfurreducens* can grow with oxygen as a terminal electron acceptor, *Appl. Environ. Microbiol. 70*, 2525−2528.
12. Way, S. S., Sallustio, S., Magliozzo, R. S., and Goldberg, M. B. (1999) Impact of either elevated or decreased levels of cytochrome *bd* expression on *Shigella flexneri* virulence, *J. Bacteriol. 181*, 1229.
13. Endley, S., McMurray, D., and Ficht, T. A. (2001) Interruption of the *cydB* locus in *Brucella abortus* attenuates intracellular survival and virulence in the mouse model of infection, *J. Bacteriol. 183*, 2454−2462.
14. Shi, L., Sohaskey, C. D., Kana, B. D., Dawes, S., North, R. J., Mizrahi, V., and Gennaro, M. L. (2005) Changes in energy metabolism of *Mycobacterium tuberculosis* in mouse lung and under *in vitro* conditions affecting aerobic respiration, *Proc. Natl. Acad. Sci. U.S.A. 102*, 15629−15634.
15. Miller, M. J., and Gennis, R. B. (1983) The purification and characterization of the cytochrome *d* terminal oxidase complex of the *Escherichia coli* aerobic respiratory chain, *J. Biol. Chem. 258*, 9159−9165.
16. Mogi, T., Mizuochi-Asai, E., Endou, S., Akimoto, S., and Nakamura, H. (2006) Role of a putative third subunit YhcB on

the assembly and function of cytochrome *bd*-type ubiquinol oxidase from *Escherichia coli*, *Biochim. Biophys. Acta 1757*, 860−864.

17. Tsubaki, M., Hori, H., and Mogi, T. (2000) Probing molecular structure of dioxygen reduction site of bacterial quinol oxidases through ligand binding to the redox metal centers, *J. Inorg. Biochem. 82*, 19−25.
18. Fang, G. H., Lin, R. J., and Gennis, R. B. (1989) Location of heme axial ligands in the cytochrome *d* terminal oxidase complex of *Escherichia coli* determined by site-directed mutagenesis, *J. Biol. Chem. 264*, 8026−8032.
19. Kaysser, T. M., Ghaim, J. B., Georgiou, C., and Gennis, R. B. (1995) Methionine-393 is an axial ligand of the heme b_{558} component of the cytochrome *bd* ubiquinol oxidase from *Escherichia coli*, *Biochemistry 34*, 13491−13501.
20. Pearson, M. A., Reczek, D., Bretscher, A., and Karplus, P. A. (2000) Structure of the ERM protein moesin reveals the FERM domain fold masked by an extended actin binding tail domain, *Cell 101*, 259−270.
21. Jünemann, S., and Wrigglesworth, J. M. (1994) Antimycin inhibition of the cytochrome *bd* complex from *Azotobacter vinelandii* indicates the presence of a branched electron transfer pathway for the oxidation of ubiquinol, *FEBS Lett. 345*, 198−202.
22. Jünemann, S., Wrigglesworth, J. M., and Rich, P. R. (1997) Effects of decyl-aurachin D and reversed electron transfer in cytochrome *bd*, *Biochemistry 36*, 9323−9331.
23. Poole, R. K., and Williams, H. D. (1987) Proposal that the function of the membrane-bound cytochrome a_1-like haemoprotein (cytochrome *b*-595) in *Escherichia coli* is a direct electron donation to cytochrome *d*, *FEBS Lett. 217*, 49−52.
24. Hill, B. C., Hill, J. J., and Gennis, R. B. (1994) The room temperature reaction of carbon monoxide and oxygen with the cytochrome *bd* quinol oxidase from *Escherichia coli*, *Biochemistry 33*, 15110−15115.
25. Kobayashi, K., Tagawa, S., and Mogi, T. (1999) Pulse radiolysis studies on electron transfer processes in cytochrome *bd*-type ubiquinol oxidase from *Escherichia coli*, *Biochemistry 38*, 5913−5917.
26. Hori, H., Tsubaki, M., Mogi, T., and Anraku, Y. (1996) EPR study of NO complex of *bd*-type ubiquinol oxidase from *Escherichia coli*. The proximal ligand of heme *d* is a nitrogenous amino acid residue, *J. Biol. Chem. 271*, 9254−9258.
27. Hill, J. J., Alben, J. O., and Gennis, R. B. (1993) Spectroscopic evidence for a heme-heme binuclear center in the cytochrome *bd* ubiquinol oxidase from *Escherichia coli*, *Proc. Natl. Acad. Sci. U.S.A. 90*, 5863−5867.
28. Borisov, V. B., Liebl, U., Rappaport, F., Martin, J., Zhang, J., Gennis, R. B., Konstantinov, A. A., and Vos, M. H. (2002) Interactions between heme *d* and heme b_{595} in quinol oxidase *bd* from *Escherichia coli:* A photoselection study using femtosecond spectroscopy, *Biochemistry 41*, 1654−1662.
29. Hirota, S., Mogi, T., Ogura, T., Anraku, Y., Gennis, R. B., and Kitagawa, T. (1995) Resonance Raman study on axial ligands of heme irons in cytochrome *bd*-type ubiquinol oxidase from *Escherichia coli*, *Biospectroscopy 1*, 305−311.
30. Sun, J., Kahlow, M. A., Kaysser, T. M., Osborne, J., Hill, J. J., Rohlfs, R. J., Hille, R., Gennis, R. B., and Loehr, T. M. (1996) Resonance Raman spectroscopic identification of a histidine ligand of b_{595} and the nature of the ligation of chlorin *d* in the fully reduced *Escherichia coli* cytochrome *bd* oxidase, *Biochemistry 35*, 2403−2412.
31. Jiang, F. S., Zuberi, T. M., Cornelius, J. B., Clarkson, R. B., Gennis, R. B., and Belford, R. L. (1993) Nitrogen and proton ENDOR of cytochrome *d*, hemin, and metmyoglobin in frozen solutions, *J. Am. Chem. Soc. 115*, 10293−10299.
32. Ingledew, W. J., Rothery, R. A., Gennis, R. B., and Salerno, J. C. (1992) The orientation of the three haems of the '*in situ*' ubiquinol oxidase, cytochrome *bd*, of *Escherichia coli*, *Biochem. J. 282*, 255−259.
33. Kranz, R. G., and Gennis, R. B. (1984) Characterization of the cytochrome *d* terminal oxidase complex of *Escherichia coli* using polyclonal and monoclonal antibodies, *J. Biol. Chem. 259*, 7998−8003.
34. Dueweke, T. J., and Gennis, R. B. (1990) Epitopes of monoclonal antibodies which inhibit ubiquinol oxidase activity of *Escherichia coli* cytochrome *d* complex localize functional domain, *J. Biol. Chem. 265*, 4273−4277.
35. Lorence, R. M., Carter, K., Gennis, R. B., Matsushita, K., and Kaback, H. R. (1988) Trypsin proteolysis of the cytochrome *d* complex of *Escherichia coli* selectively inhibits ubiquinol oxidase activity while not affecting *N*,*N*,*N*′,*N*′-tetramethyl-p-phenylenediamine oxidase activity, *J. Biol. Chem. 263*, 5271−5276.
36. Dueweke, T. J., and Gennis, R. B. (1991) Proteolysis of the cytochrome *d* complex with trypsin and chymotrypsin localizes a quinol oxidase domain, *Biochemistry 30*, 3401−3406.
37. Matsumoto, Y., Murai, M., Fujita, D., Sakamoto, K., Miyoshi, H., Yoshida, M., and Mogi, T. (2006) Mass spectrometric analysis of the ubiquinol-binding site in cytochrome *bd* from *Escherichia coli*, *J. Biol. Chem. 281*, 1905−1912.
38. Mogi, T., Akimoto, S., Endou, S., Watanabe-Nakayama, T., Mizuochi-Asai, E., and Miyoshi, H. (2006) Probing the ubiquinol-binding site in cytochrome *bd* by site-directed mutagenesis, *Biochemistry 45*, 7924−7930.
39. Zhang, J., Hellwig, P., Osborne, J. P., Huang, H., Moenne-Loccoz, P., Konstantinov, A. A., and Gennis, R. B. (2001) Site-directed mutation of the highly conserved region near the Q-loop of the cytochrome *bd* quinol oxidase from *Escherichia coli* specifically perturbs heme b_{595}, *Biochemistry 40*, 8548−8556.
40. Green, G. N., Kranz, R. G., Lorence, R. M., and Gennis, R. B. (1984) Identification of subunit I as the cytochrome b_{558} component of the cytochrome *d* terminal oxidase complex of *Escherichia coli*, *J. Biol. Chem. 259*, 7994−7997.
41. Tsubaki, M., Hori, H., Mogi, T., and Anraku, Y. (1995) Cyanide-binding site of *bd*-type ubiquinol oxidase from *Escherichia coli*, *J. Biol. Chem. 270*, 28565−28569.
42. Sakamoto, K., Miyoshi, H., Takegami, K., Mogi, T., Anraku, Y., and Iwamura, H. (1996) Probing substrate binding site of the *Escherichia coli* quinol oxidases using synthetic ubiquinol analogues based upon their electron-donating efficiency, *J. Biol. Chem. 271*, 29897−29902.
43. Ito, M., Matsuo, Y., and Nishikawa, K. (1997) Prediction of protein secondary structure using the 3D-1D compatibility algorithm, *Comput. Appl. Biosci. 13*, 415−424.
44. Matsumoto, Y., Muneyuki, E., Fujita, D., Sakamoto, K., Miyoshi, H., Yoshida, M., and Mogi, T. (2006) Kinetic mechanism of quinol oxidation by cytochrome *bd* studied with ubiquinone-2 analogs, *J. Biochem. 139*, 779−788.
45. Azarkina, N., Siletsky, S., Borisov, V., von Wachenfeldt, C., Hederstedt, L., and Konstantinov, A. A. (1999) A cytochrome *bb*′-type quinol oxidase in *Bacillus subtilis* strain 168, *J. Biol. Chem. 274*, 32810−32817.
46. Cunninghams, L., Pitt, M., and Williams, H. D. (1997) The *cioAB* genes from *Pseudomonas aeruginosa* code for a novel cyanide-insensitive terminal oxidase related to the cytochrome *bd* quinol oxidases, *Mol. Microbiol. 24*, 579−591.
47. Berry, S., Schneider, D., Vermaas, W. F. J., and Rögner, M. (2002) Electron transport routes in whole cells of *Synechocystis* sp. strain PCC 6803: The role of the cytochrome *bd*-type oxidase, *Biochemistry 41*, 3422−3429.
48. Zhang, J., Hellwig, P., Osborne, J. P., and Gennis, R. B. (2004) Arginine 391 in subunit I of the cytochrome *bd* quinol oxidase from *Escherichia coli* stabilizes the reduced form of the hemes and is essential for quinol oxidase activity, *J. Biol. Chem. 279*, 53980−53987.
49. Belevich, I., Borisov, V. B., Zhang, J., Yang, K., Konstantinov, A. A., Gennis, R. B., and Verkhovsky, M. I. (2005) Time-resolved electrometric and optical studies on cytochrome *bd* suggest a mechanism of electron-proton coupling in the di-heme active site, *Proc. Natl. Acad. Sci. U.S.A. 102*, 3657−3662.
50. Yamazaki, Y., Kandori, H., and Mogi, T. (1999) Fourier-transform infrared studies on conformational changes of *bd*-type ubiquinol oxidase from *Escherichia coli* upon photoreduction of the redox metal centers, *J. Biochem. 125*, 1131−1136.
51. Oden, K. L., and Gennis, R. B. (1991) Isolation and characterization of a new class of cytochrome *d* terminal oxidase mutants of *Escherichia coli*, *J. Bacteriol. 173*, 6174−6183.
52. Ghaim, J. B., Greiner, D. P., Meares, C. F., and Gennis, R. B. (1995) Proximity mapping the surface of a membrane protein using an artificial protease: Demonstration that the quinone-binding domain of subunit I is near the N-terminal region of subunit II of cytochrome *bd*, *Biochemistry 34*, 11311−11315.

BI0615792